REPORT DOCUMENTATION PAGE

AFRL-SR-BL-TR-00-

0526

1. REPORT DATE *(DD-MM-YYYY)*
21 Sep 2000

2. REPORT TYPE
Final Technical

3. DATES COVERED *(From - To)*
01 Mar 1998 to 29 Feb 2000

4. TITLE AND SUBTITLE
MOCVD Upgrade

5a. CONTRACT NUMBER

5b. GRANT NUMBER
F49620-98-1-0296

5c. PROGRAM ELEMENT NUMBER

5d. PROJECT NUMBER

5e. TASK NUMBER

5f. WORK UNIT NUMBER

6. AUTHOR(S)
Julian Cheng

7. PERFORMING ORGANIZATION NAME(S) AND ADDRESS(ES)
The University of New Mexico
Center for High Technology
Materials
1313 Goddard SE
Albuquerque, NM 87106

8. PERFORMING ORGANIZATION REPORT NUMBER 310661 FT-1

9. SPONSORING / MONITORING AGENCY NAME(S) AND ADDRESS(ES)
Air Force Office
Of Scientific Research
801 North Randolph St. Room 732
Ballston Tower II
Arlington, VA 22203-1977

10. SPONSOR/MONITOR'S ACRONYM(S)
AFOSR/NE

11. SPONSOR/MONITOR'S REPORT NUMBER(S)

12. DISTRIBUTION / AVAILABILITY STATEMENT
Unlimited

20001023 059

13. SUPPLEMENTARY NOTES

14. ABSTRACT

The goal of this research program is to develop a novel technology for the epitaxial growth and fabrication of vertical-cavity surface-emitting laser structures with lasing wavelengths in the 110 nm to 1500 nm regime, with special emphasis on the 1300 nm VCSEL's and monolithic VCSEL arrays. These are useful for the parallel optical data links that will interconnect future computer networks, whose nodes may be distributed across a wide range of distances and are interconnected by optical fibers. The use of 1300nm VCSEL's will provide improved fiber transmission performance as well as a more unified technology platform for the different levels of the interconnect hierarchy. The GaInNAs/GaAs VCSEL technology represents a novel approach that is potentially manufacturable using conventional growth systems and device fabrication techniques.

15. SUBJECT TERMS
Optoelectronics, MOCVD

16. SECURITY CLASSIFICATION OF: a. REPORT	b. ABSTRACT	c. THIS PAGE	17. LIMITATION OF ABSTRACT	18. NUMBER OF PAGES	19a. NAME OF RESPONSIBLE PERSON
Unclassified	Unclassified	Unclassified	UNL	13	Julian Cheng
					19b. TELEPHONE NUMBER *(include area code)* (505) 272-7846

MOCVD Upgrade

Julian Cheng
Principal Investigator

University of New Mexico
Center for High Technology Materials
1313 Goddard SE
Albuquerque, NM 87106

Phone: 505-272-7846
Fax: 505-272-7801
E-mail: cheng@chtm.unm.edu

Final Report to

Air Force Office of Scientific Research

Under

Grant # F49620-98-1-0296

DATE: September 21, 2000

1. Statement of Work (SOW)

The goal of this research program is to develop a novel technology for the epitaxial growth and fabrication of vertical-cavity surface-emitting laser structures with lasing wavelengths in the 1100 nm to 1500 nm regime. Special emphasis will be on the realization of 1300 nm VCSELs and monolithic VCSEL arrays, which are useful for the parallel optical data links that will interconnect future computer networks, whose nodes may be distributed across a wide range of distances and are interconnected by optical fibers. The use 1300 nm VCSELs will provide improved fiber transmission performance as well as a more unified technology platform for the different levels of the interconnect hierarchy. We will design and demonstrate a practical 1300 nm VCSEL structure that can be grown by a single epitaxial growth on a conventional GaAs substrate. These structures will contain a GRINSCH active region with one or more strain-compensated InGaAsN quantum wells, as well as IGaAs/AlAs distributed Bragg reflector (DBR) mirrors with a large index difference, which allows the total thickness of each mirror to be reduced and thus manageable from the crystal growth standpoint. We will develop an optimum device design for the fabrication of these VCSEL structures, and integrate them into monolithic arrays.

2. Introduction

Long wavelength VCSEL-based optical Interconnect and optical networking technologies will have important applications in future computer networks, including the Internet. They provide a common technology for local optical interconnects, backplanes, LANs and switched hubs that will one day provide a seamless optical network at all levels of the interconnection hierarchy, bringing broadband ISDN and the global optical information network to the desktop. At present there is no all-epitaxially-grown long wavelength VCSEL technology, nor is there any other approach with proven performance or reliability. The proposed GaInNAs/GaAs VCSEL technology represents a novel approach that is potentially manufacturable using conventional growth systems and device fabrication techniques.

2(a). Long-Wavelength Vertical-Cavity Surface-Emitting Lasers

Although VCSEL development in the 850 nm (GaAs/AlGaAs) to 980 nm (InGaAs/AlGaAs) wavelength regime has proceeded apace, there has been little progress in the development of longer wavelength VCSELs in the 1.30 μm and 1.55 μm region due to problems in epitaxial growth. Since the thickness of the distributed Bragg reflector mirror (DBR, which consists of many pairs of quarter-wavelength-thick, high-index and low-index layers) and the thickness of the active region both scale with wavelength, the total growth thickness of a long wavelength VCSEL at λ=1.30 μm and at λ=1.54 μm will be 52% and 81% thicker, respectively, than a VCSEL operating at λ=850 nm. Moreover, the maximum index difference between the high-index (InGaAsP) and low-index (InP or InAlGaAs) layers of the DBR stack is smaller ($\Delta n \sim 0.25$) in the InGaAsP/InP or InGaAlAs/InP material system, compared to $\Delta n \sim 0.5$ for an AlGaAs/GaAs DBR. Therefore many more DBR pairs will be needed to achieve the high reflectivity (R>0.998) that is required for lasing, which further exacerbates the thickness requirement (~20 μm). Thus a long-wavelength (InGaAsP/InP) VCSEL structure cannot be easily realized by epitaxial growth alone.

2(b). Single-Growth Long Wavelength Lasers:

A single-epitaxial-growth approach would be the ideal solution to the long-wavelength VCSEL problem. *At present, there is no all-epitaxially-grown long wavelength VCSEL technology* with proven performance or reliability. As a result of these considerations, the approaches that we have selected are all based on: (1) a single epilayer growth, (2) simple, conventional GaAs/AlGaAs VCSEL fabrication technology, (3) GaAs/AlGaAs DBR mirrors, (4) no wafer fusion or any other additional processing technologies. We have looked at three different approaches to a 1.3 μm VCSEL structure that are based on three different material systems, which included: (1) strain-compensated InGaAs quantum wells with GaAsP barrier layers grown on a ternary InGaAs substrate, (2) GaInNAs/GaAs quantum wells grown on a GaAs substrate, and (3) InAs/InGaAs quantum dot-in-well layers grown on a GaAs substrate. We have made very substantial progress in developing the latter two approaches, and have achieved state-of-the-art long wavelength lasers based on GaInNAs and the InAs quantum dots. We have also made lasers grown on the ternary substrates, but the quality of the substrates that we have obtained from Johnson-Matthey were not of sufficiently high quality to produce high-performance lasers.

The new approach uses a novel narrow-bandgap material - InGaAsN lattice-matched to GaAs - as the active region, and utilizes the larger index difference of the conventional AlGaAs/AlAs DBRs. It offers a structural simplicity that makes VCSELs far easier to fabricate than approaches that require the wafer bonding of one or more GaAs/AlGaAs DBRs to an InGaAsP/InP active region. Our first objective is to investigate the use of $In_xGa_{1-x}As_{1-y}N_y$, to achieve 1.3 VCSEL operation on a GaAs substrate. The goal is to develop a practical and potentially manufacturable new VCSEL technology that is based on a single-growth using conventional growth systems, using only conventional substrates and established device fabrication techniques.

2©. 1.3 μm VCSELs using $In_xGa_{1-x}As_{1-y}N_y$ active layers grown on GaAs Substrates

Fig. 1 shows the bandgap energy as a function of lattice constant for a variety of III-V compound semiconductor materials. Due to the large electronegativity of nitrogen atoms, a negative bandgap energy has been predicted for N-containing compounds such as $GaAs_{1-x}N_x$, $GaP_{1-x}N_x$, and $AlAs_{1-x}N_x$. This huge bowing of bandgap energy provides another degree of freedom in bandgap engineering by providing novel material systems that can be exploited to realize long-wavelength lasers or other electronic devices on GaAs substrates. For example, adding 10% In to GaAs increases the lattice constant of the $In_{0.1}Ga_{0.9}As$ layer, placing it under compressive strain, while adding approximately 2% N to the $In_{0.1}Ga_{0.9}As$ layer decreases its lattice constant and thus compensates for the compressive strain. Thus a strain-free material, $In_xGa_{1-x}As_{1-y}N_y$ grown on GaAs, can be easily obtained by choosing suitable compositions x and y. Furthermore, due to this unique bandgap bowing effect, the bandgap energy of In_xGa_{1-}

${}_xAs_{1-y}N_y$ can be significantly reduced below that of GaAs. The bandgap energy of $In_{0.1}Ga_{0.9}As_{0.98}N_{0.02}$ (E_3) is much smaller than that of $In_{0.1}Ga_{0.9}As$ (E_1) or $GaAs_{0.98}N_{0.02}$ (E_2). This result strongly suggests that the $In_xGa_{1-x}As_{1-y}N_y$ alloy has a great potential for long-wavelength laser applications. Much better electron confinement can therefore be obtained, thus significantly reducing the carrier leakage. The AlGaAs/GaAs DBRs are transparent to the luminescence of the $In_xGa_{1-x}As_{1-y}N_y/Al_xGa_{1-x}As$ quantum wells.

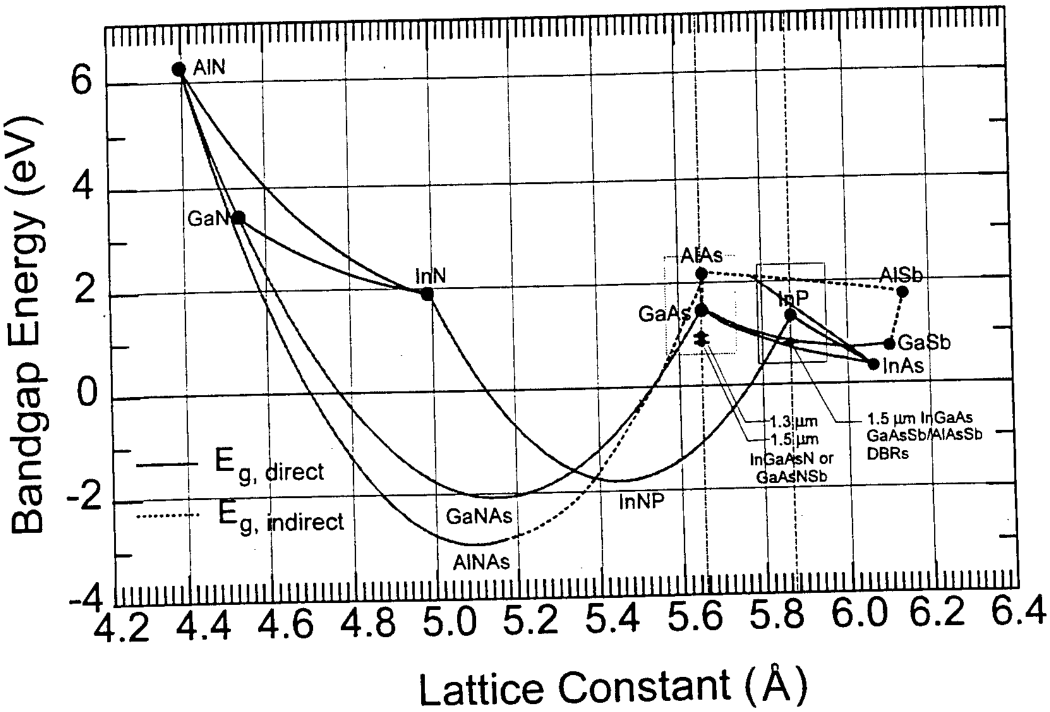

Fig. 1 The composition dependence of the bandgap energies of III-NAs and III-NP alloys calculated based on the Van Vechten model. The boxes indicate two different material systems that can be used to achieve long wavelength VCSELs.

2(d). MOCVD Sources for the growth of $In_xGa_{1-x}As_{1-y}N_y$ Materials:

From the above discussions, we can identify that one important material issue, how to achieve enough N incorporation in $In_xGa_{1-x}As_{1-y}N_y$, which must be addressed first before long wavelength VCSELs can be realized. The growth of $In_xGa_{1-x}As_{1-y}N_y$ on GaAs substrates generally requires a lower growth temperature, typically 450-650°C, in order to achieve a reasonable N incorporation in GaAs. The incorporation efficiency of N in these materials is found to increase with decreasing growth temperatures. Therefore an effective N-source that is suitable for low temperature (~ 400-500°C) growth would be highly desirable. The approach that we have adopted is to grow compressively-strained GaInAsN quantum wells using MOCVD by increasing the In concentration instead of the N concentration, which happily also results in highly epilayer material quality and higher luminescence efficiency as a result of the lower N content.

3. Efficient Continuous-Wave Lasing Operation of a Narrow-Stripe Oxide-Confined GaInNAs/GaAs Multi-Quantum Well Laser Grown by MOCVD

Efficient cw lasing operation has been achieved above room temperature by a triple-quantum well GaInNAs/GaAs laser diode grown on a 6°-misoriented GaAs substrate by MOCVD. Using a planar, oxide-confined, narrow-stripe (8 μm) laser geometry, continuous-wave lasing operation was achieved over a wide range of temperatures up to 57 °C. At room temperature, lasing occurs at a wavelength of 1.16 μm, with a high single-facet slope efficiency of 25% and a threshold current density of 1.3 kA/cm^2.

The GaInNAs/GaAs material system represents a promising single-epitaxial-growth approach for achieving long wavelength (1.3 μm) vertical-cavity surface-emitting lasers (VCSEL's) on a conventional GaAs substrate [1], as well as edge-emitting lasers with a high characteristic temperature T_o. The growth of GaInNAs quantum wells on GaAs substrates can take advantage of the larger refractive index difference of AlGaAs/AlAs-based distributed Bragg reflector (DBR) mirrors to grow VCSELs with a more tractable total thickness, which is a distinct advantage over the use of InP-based DBR structures. Compared to the long wavelength laser diodes based on GaInAsP alloys, the GaInNAs/AlGaAs-based laser structures can provide better electron confinement, giving rise to a larger T_o and reduced temperature sensitivity for the laser [1-4]. The value of T_o has previously been determined to be ~125 K, which was obtained mostly under pulsed lasing operation. The lowest threshold current density for pulsed lasing operation was achieved at 1.28 μm by a single-quantum well (SQW) laser with a threshold current density of J_{th} = 800 A/cm^2 [5], and at 1.17 μm by a 3QW laser with a current density of 667 A/cm^2 [6]. Until recently, cw lasing for GaInNAs lasers has only been achieved at room temperature by a SQW, 1.3 μm laser grown by MBE [7], with J_{th}= 6.3 kA/cm^2, and by a two-QW, 1.3 μm ridge waveguide laser grown by MOCVD [8], the latter with J_{th}= 1.2 kA/cm^2. In order to achieve efficient cw lasing operation over a wide range of temperatures above room temperature, the operating current must be reduced by decreasing the width of the active region to much smaller dimensions. A simple means for achieving this while maintaining planarity and minimizing the effects of lateral current spreading is to confine the current to a small active area aperture by using the lateral wet oxidation of one or more $Al_{0.98}Ga_{0.02}As$ layers that are adjacent to the active layer [9,10]. This technique is readily scaleable to active area dimensions as small as 2 μm.

The efficient room-temperature cw lasing operation of a 3QW GaInNAs edge-emitting laser has been achieved for the first time using a lateral oxide-confinement design. The cw lasing operation was achieved over a wide range of temperatures (up to 57°C), with reasonably low threshold current density (0.98 kA/cm^2 at 0 °C, and 1.3 kA/cm^2 at 23 °C), high slope efficiency (28.5 % per facet at 0°C, 25 % at 23 °C) for devices with a narrow stripe width (8 μm). CW lasing occurs at room temperature with an emission wavelength of ~1.16 μm, a threshold current of 76 mA (J_{th} = 1.3 kA/cm^2), and a high single-facet slope efficiency of 25%.

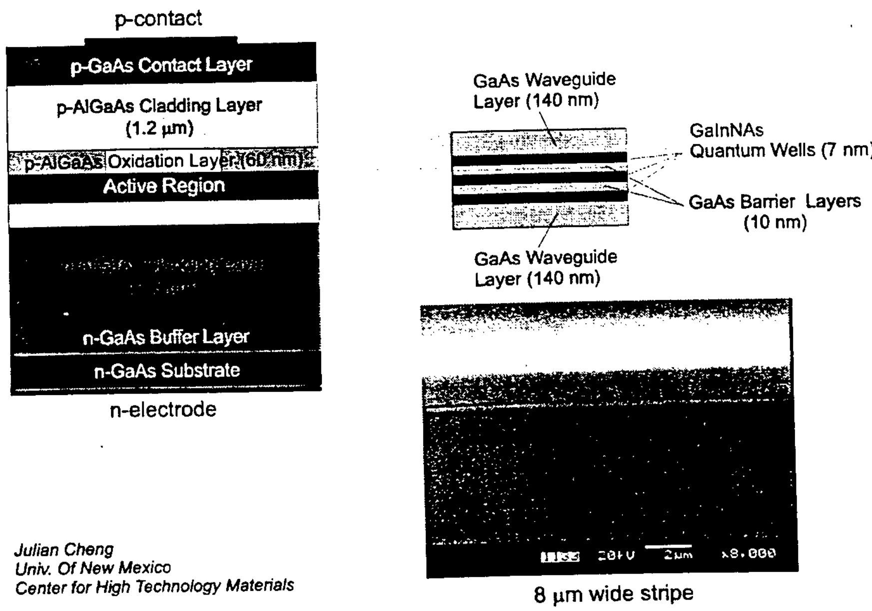

Fig. 2. The epilayer structure and device design of a 3 QW GaInNAs/GaAs laser.

The device design is shown in figure 2. The active region of the laser diode consists of three 7 nm thick $Ga_{0.7}In_{0.3}N_{0.003}As_{0.997}$ quantum wells separated by 10 nm thick GaAs barrier layers, and is bounded on either side by a 140 nm thick undoped GaAs waveguide layer. These are in-turn bounded by p-doped and n-doped $Al_{0.3}Ga_{0.7}As$ cladding layers with a thickness of 1.2 μm and 1.5 μm, respectively, and a thin $Al_{0.98}Ga_{0.02}As$ selective oxidation layer was added at each GaAs/AlGaAs heterointerface. The epilayer structure was grown by MOCVD on n-type (100) GaAs substrates that are misoriented by 6° towards [111]A, which have demonstrated superior photoluminescence (~30% higher radiative efficiency) compared to structures grown on 0°-off substrates [6]. The growth was performed by low pressure MOCVD using dimethylhydrazine (DMHy) as the nitrogen source, and the growth conditions have been described elsewhere [11].

The lasers were fabricated by first patterning and depositing the Ti/Pt/Au p-contact metal stripes (65 μm wide), then dry etching 91μm-wide mesas down to the substrate, and using selective lateral wet oxidation of the two $Al_{0.98}Ga_{0.02}As$ layers adjacent to the active region to define oxide layers that effectively confine the current to a small active area aperture (8 μm wide). The substrate was then thinned to a thickness of ~120 μm, and AuGe/Ni/Au n-contact metal was deposited on the back substrate surface. The samples were cleaved into bars 720 μm in length and were bonded onto copper heat sinks prior to device characterization.

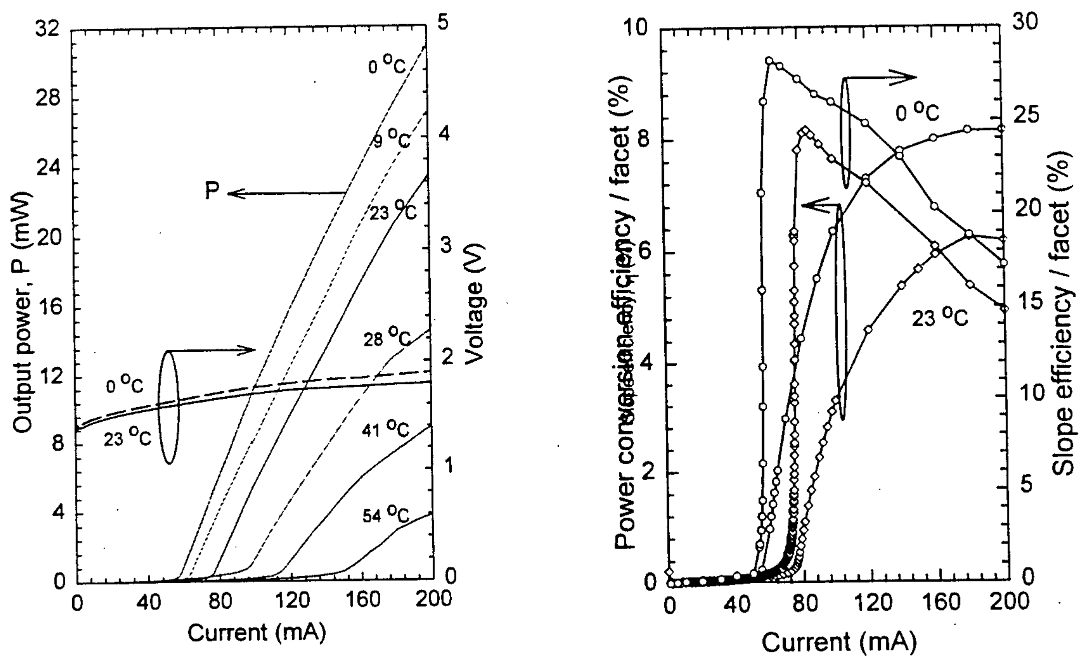

Figure 3. a) CW output power and voltage versus current for a narrow-stripe oxide-confined laser diode (L = 720 μm, W = 8 μm) at various temperatures. b) Single facet power conversion efficiency and slope efficiency for the same laser diode at 0 °C and 23 °C.

The electrical and cw lasing characteristics of a narrow-stripe oxide-confined GaInNAs laser (L = 720 μm long, W = 8 μm wide) at temperatures ranging from 0°C to 54 °C are shown in Fig. 3. The characteristics at room temperature show a threshold current of 76 mA (J_{th} = 1.3 kA/cm^2), a threshold voltage of 1.70 V, a single-facet slope efficiency of 25% and a single-facet power conversion efficiency of 6.3%, and an output power of 23 mW at a bias current of 200 mA. The corresponding parameters for 0 °C operation are 57 mA (J_{th} = 0.98 kA/cm^2), 1.66 V, 28.5%, 8.1%, and 31 mW, respectively. The threshold current increases with temperature, and cw lasing is observed over a wide temperature range up to 57 °C. The device also shows good dc electrical characteristics, with a turn-on voltage of 1.35 V and a very low series resistance of 2 Ω. The operating voltage of the laser diode remains less than 2 V for drive currents up to 200 mA throughout the entire temperature range from 0 °C to 54 °C. Figure 4 plots the inverse external slope efficiency (for both facets) as a function of the cavity length for a number of different GaInNAs lasers under cw lasing operation. From the slope and the y-axis intercept, the internal optical loss (α_i =4.2 cm^{-1}) and internal quantum efficiency (η_i=0.64) have been calculated. Excellent electrical and cw lasing performance has thus been achieved for the first time by a MOCVD-grown GaInNAs laser with an oxide-confined stripe width below 10 μm, with low threshold current density, low operating voltage, high differential slope efficiency and power conversion efficiency, and a wide temperature range for cw lasing operation.

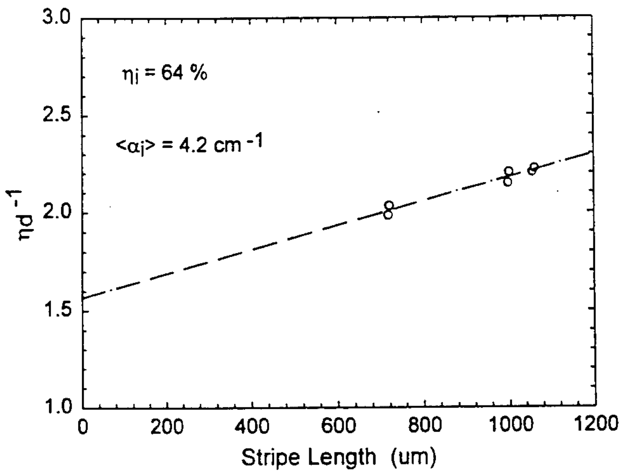

Figure 4. The inverse external slope efficiency of a GaInNAs Laser (both facets) as a function of the cavity length at room temperature. From the slope and the y-axis intercept, the optical loss (α_i = 4.2 cm^{-1}) and the internal quantum efficiency (η_i = 0.64) have been calculated.

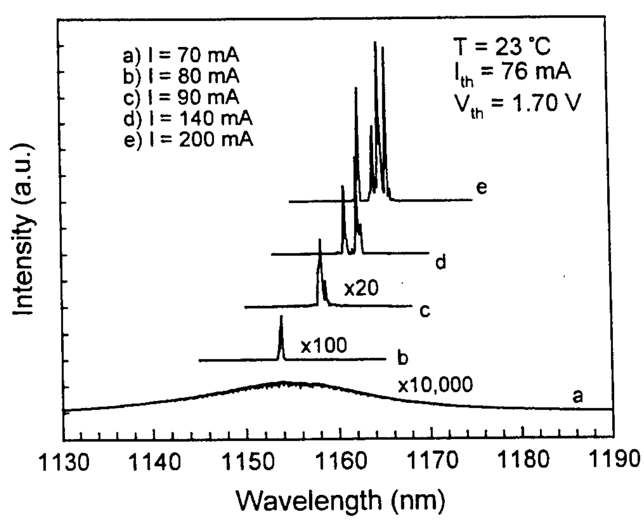

Figure 5. Emission spectra of the GaInNAs/GaAs MQW laser diode under cw operation at room temperature with different drive currents.

Figure 5 shows the room temperature cw lasing spectra of the GaInNAs MQW laser under different bias currents. The lasing spectrum is single mode at bias currents up to $I=1.2\times I_{th}$, with a side mode suppression ratio (SMSR) of ~20 dB. The peak emission wavelength of the laser diode is 1.154 μm near threshold, and shifts to a longer wavelength with increasing drive current. At bias currents above 90 mA, two or more lasing modes occur. These represent different transverse modes with a wavelength spacing of ~2 nm, which is consistent with the transverse dimension of the cavity that is defined by the etched mesa (91 μm).

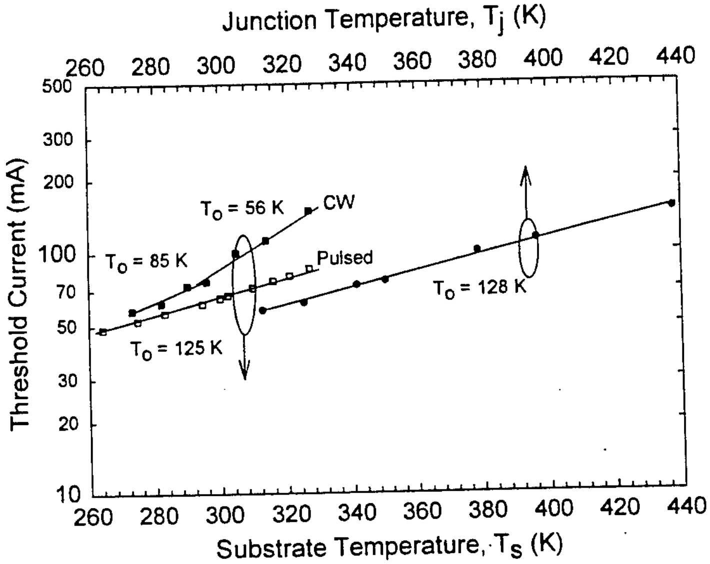

Figure 6. Temperature dependence of threshold current for the GaInNAs/GaAs MQW laser under cw and pulsed operations.

Finally, the temperature dependence of the lasing characteristics has been studied. Figure 6 plots the logarithm of the threshold current I_{th} for both pulsed and cw lasing as a function of the substrate temperature T_s, from which the characteristic temperature T_o is determined according to the relation: $I_{th} = I_o \exp(T_s/T_o)$. For pulsed lasing operation, the fit is linear and yields a T_o of 125 K. However for cw operation the fit is nonlinear, giving a value of T_o that varies from ~85 K at lower temperatures to ~56 K at higher temperatures. It can be shown that most of this non-linearity is due to thermal self-heating, which raises the junction temperature T_j substantially above the measured ambient temperature T_s. The rise in junction temperature ($\Delta T_j = T_j - T_s$) is governed by $\Delta T_j = R_{th}\times P_d$, where R_{th} is the thermal resistance and P_d is the measured power dissipation. The value of R_{th} (420 K/W) is obtained by measuring the shift in emission wavelength $\Delta\lambda$ with increasing power dissipation P_d (*i.e.*, by increasing the bias current), and relating ΔT_j to $\Delta\lambda$ using the known temperature dependence of the bandgap wavelength ($d\lambda/dT$~0.48 nm/K [1]), which is corroborated by the measured temperature dependence of the lasing wavelength near threshold ($d\lambda/dT$ ~0.478 nm/K). After calculating the internal junction temperature T_j at threshold, log (I_{th}) is replotted as a function of T_j in Fig. 4, which shows a good linear fit over the entire range of temperature from 0°C to 54°C. From this fit, the characteristic temperature (T_0) is calculated to be 128 K, which is in close agreement with the value (125 K) derived from the pulsed lasing measurements. This shows that the reduction of T_0 for cw lasing is primarily due to thermal self heating caused by a relatively high thermal resistance, which can be substantially reduced using better packaging to achieve a T_0 that is closer to its intrinsic value of 125 K to improve high temperature performance.

In conclusion, we have experimentally demonstrated, for the first time, the efficient cw lasing operation of a MOCVD-grown, narrow-stripe, oxide-confined MQW GaInNAs laser diode (L = 720 μm, W = 8 μm) at temperatures up to 57 °C (thermal cut-off). Excellent cw device performance was achieved, including a low threshold current density (1.3 kA/cm^2), low operating voltage (<1.7V), high differential slope efficiency (~50% for both facets at 23 °C) and power conversion efficiency (13% for both facets at 23 °C), and a wide temperature range for cw operation (up to 57 °C).

4. GaInNAs VCSELs

During our development of the GaInNAs/GaAs into a high-quality device-quality material system, efforts were made towards the growth of a complete GaInNAs VCSEL structure. Because of its longer wavelength, the GaInNAs VCSEL is a relatively thick structure requiring a long epitaxial growth. Most of our work had focused on GaInNAs compositions that centered at a wavelength of 1.15 μm. These structures were generally undoped since the growth of the GaInNAs quantum wells at a reduced temperature resulted in a very much enhanced memory effect from the Tellurium dopant that greatly decreased the radiative efficiency of the QWs. Figure 7 shows the photoreflectance spectrum of a GaInNAs VCSEL that was designed for 1.15 μm operation (1.13 μm experimentally measured), while figure 8 shows the optically pumped photoluminescence spectrum of this structure.

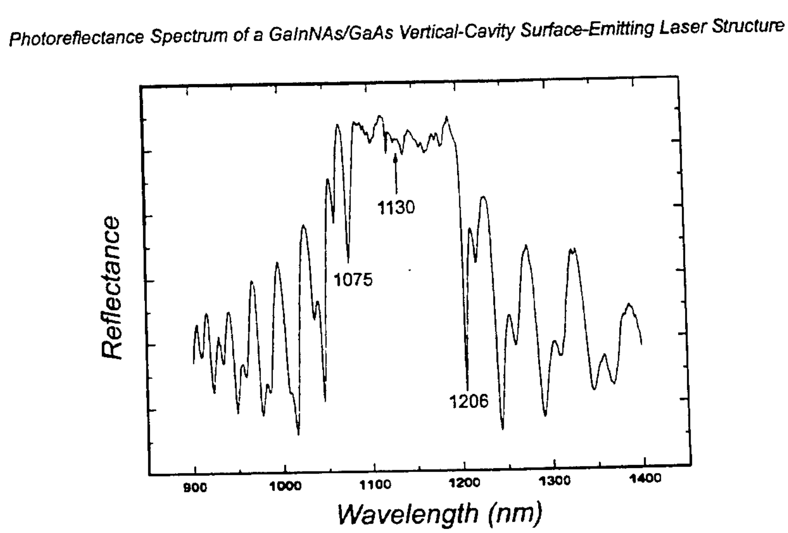

Fig. 7. The photoreflectance of a 1.15 μm VCSEL with three GaInNAs/GaAs quantum wells, showing a passband that is characteristic of the GaAs/AlAs DBR mirrors.

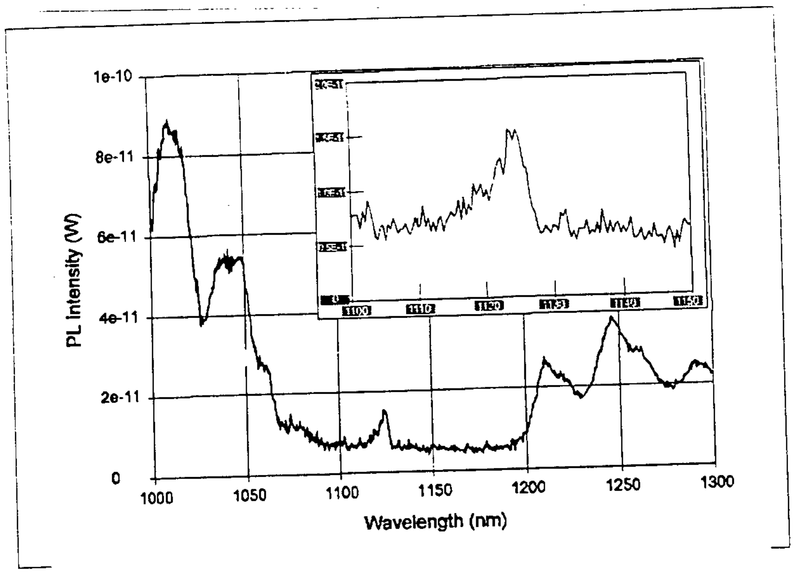

Figure 8. The photoluminescence spectrum of a GaInNAs/GaAs VCSEL.

Our experience has shown that the relatively thick, long wavelength GaInNAs VCSEL structure can be grown by MOCVD in a fairly easy and straightforward manner, and the deleterious effect of the tellurium memory on the QW's can be overcome using special growth techniques. The main obstacle to achieving a 1.3 μm VCSEL lies in our ability to push the Indium or Nitrogen composition high enough, and the bandgap small enough, to achieve a 1.3 μm gain spectrum without incurring excess lattice strain. This too can be achieved by using strain compensation if necessary.

References:

[1] M. Kondow, T. Kitatani, S. Nakatsuka, M.C. Larson, K. Nakahara, Y.Yazawa, and M. Okai, "GaInNAs: a noval material for long-wavelength semiconductor lasers", IEEE J. Slect. Topics Quantum Electron., vol. 3, pp. 719-730, 1997.

[2] S. Sato, and S. Satoh, "Room temperature pulsed operation of strained GaInNAs/GaAs double quantum well laser diode grown by metal organic chemical vapour deposition", Electron. Lett., vol. 34, pp. 1495-1497, 1998.

[3] M. Kondow, S. Nakatsuka, T. Kitatani, Y. Yazawa, and M. Okai, "Room-temperature continuous wave operation of GaInNAs/GaAs laser diode", Electron. Lett., vol. 32, pp. 2244-2245, 1996.

[4] M. Kondow, S. Nakatsuka, T. Kitatani, Y. Yazawa, and M. Okai, "Room-temperature pulsed operation of GaInNAs laser diodes with excellent, high-temperature performance", Jpn. J. Appl. Phys., vol. 35, pp. 5711-5713, 1996.

[5] F. Hohnsdorf, J. Koch, S. Leu, W. Stoltz, B. Borchert, and M. Druminski, "(GaN)(InAs)/GaAs single quantum well lasers for emission wavelength in the range 1.28-1.38 μm", Electron. Lett., vol. 35, pp. 571-572, 1999.

[6] C.P. Hains, N.Y. Li, K. Yang, X.D. Huang, and J. Cheng, "Room-temperature pulsed operation of triple-quantum well GaInNAs/GaAs lasers with low threshold current density grown on misoriented GaAs substrates by MOCVD", IEEE Photonics Technol. Lett., Vol.11, pp. 1208-1210, 1999.

[7] K. Nakahara, M. Kondow, T. Kitatani, M.C. Larson, and K. Uomi, "1.3 μm continuous-wave operation in GaInNAs quantum well lasers", IEEE Photonics Technol. Lett., Vol. 10, pp. 487-488, 1998.

[8] S. Sato, S. Satoh, "1.3 μm continuous-wave operation of GaInNAs lasers grown by metal organic chemical vapour deposition", Electronics Letters, Vol.35, pp. 1251-1252, 1999

[9] J.M. Dallesasse, N. Holonyak, Jr., A. R. Sugg, T. A. Richard, and N. ElZein, "Hydrolyzation oxidation of $Al_xGa_{1-x}As$-AlAs-GaAs quantum well heterostructures and superlattices", Appl. Phys. Lett., Vol. 57, pp. 2844-2846, 1990

[10] S.A. Maranowski, A. R. Sugg, E. I. Chen, and N. Holonyak, Jr. "Native oxide top- and bottom-confined narrow stripe p-n $Al_yGa_{1-y}As$-GaAs-$In_xGa_{1-x}As$ quantum well heterostructure laser", Appl. Phys. Lett, Vol.63, pp. 1660-1662, 1993

[11] N.Y. Li, C.P. Hains, K. Yang, J. Lu, J. Cheng, and P.W. Li, "Organometallic vapor phase epitaxy growth and optical characteristics of almost 1.2 μm GaInNAs three-quantum-well laser diodes", Appl. Phys. Lett., Vol.75, pp. 1051-1053, 1999.

The University of New Mexico
Julian Cheng, Principal Investigator
F49620-98-1-0296
Final Technical Report

Equipment specifications:

Manufacturer: Thomas Swan & Co Ltd.
1) MOCVD Reactor System for Group III Nitrides and related Materials Frowth on 2 inch wafers
Price $ 149,500

Upgrade to an existing horizontal reactor on a Thomas Swan MOCVD Epitor System to a single wafer vertical reactor. The backbone of this system is comprised of two frames which include components and assemblies common to all T. Swan systems to support 1) the gas delivery system and, 2) the reactor cell and exhaust system. The computer operating system runs on a PC platform with the operating software written in "C" code running under Windows. The system includes two switching manifolds and a differential pressure control. It has standard gas lines, double dilution gas lines and an additional hydride line. The system is placed in a customized glove box with loading via a load lock. The recirculation system includes a nitrogen drier/deoxygenation column, thereby maintaining a pure atmosphere. The column also has regeneration facilities.

2) Modification of the Thomas Swan Gas Input System
Price: $10,800

Enables user to deposit GaN. Sor systems in which group III nitrides are to be grown, the input gas manifold is configured such that the carrier lines are able to transport both hydrogen or nitrogen ro a controlled mixture of both species. The facility is pres-requisite for the effective growth of some alloys.

3) Installation charge
Price: $5,500